CHAPTER 2

Electrical and Gas Sensing Properties of PQT-12 Based Metal-Semiconductor-Metal Device*

Contents

2.1 Introduction 41

2.2 Experimental Details 42

2.2.1 Materials and Thin Film Deposition 42

2.2.2 Device Fabrication 43

2.3 Results and Discussion 44

2.3.1 Thin Film Characterization 44

2.3.2 Electrical Characterization 48

2.3.3 Gas Sensing Characterization 49

2.3.3.1 Ammonia Gas Response of MSM Sensor 50

2.3.3.2 Nitrogen Dioxide Gas Response of MSM Sensor 53

2.3.3.3 Selectivity of MSM Sensor 56

2.4 Conclusion 57

*Part of this work has been published as:

1. Chandan Kumar et al., "Flexible poly(3, 3‴-dialkylquaterthiophene) based interdigitated metal-semiconductor-metal ammonia gas sensor," *Sensors & Actuators B: Chemical*, vol. 255, pp. 203–209, 2018.
2. Chandan Kumar et al., "Poly(3, 3‴-dialkylquaterthiophene) based flexible nitrogen dioxide gas sensor," *IEEE Sensors Letters*, vol. 2, no. 1, p. 4500104, 2018.

CHAPTER 2

Electrical and Gas Sensing Properties of PQT-12 Based Metal-Semiconductor-Metal Device

2.1 Introduction

Electronic gas sensors are of great importance these days for monitoring hazardous gases such as ammonia, nitrogen dioxide, carbon monoxide, hydrogen etc. in the environment, automotive industry, chemical industry and refrigeration industry [61], [62]. Both the inorganic materials (mainly metal oxides and their nanostructures) [62]–[66] and organic conducting polymers [9], [67]–[75] have been used for fabricating the gas sensors. Although, most of the commercially available gas sensors are based on metal-oxides especially using SnO_2 [76], but their poor selectivity [62], high fabrication cost due to the requirement of very expensive set up [9] and poor room temperature response have greatly encouraged for developing low-cost and low-temperature based sensors using conducting polymers [9], [67]–[75] as discussed in Chapter-1. As discussed in Chapter-1, the conducting polymer based devices could be preferred over the conventional semiconductor based devices due to their low fabrication cost owing to low-cost synthesis of polymers and their low-temperature solution based processing, large-area fabrication possibility and compatibility with plastic flexible substrates [62]. Further, the polymer based devices are inherently enviro-friendly with reasonable repetitive room temperature response [119] and high selectivity [9] as discussed in Chapter-1. Among various conducting polymers, PQT-12 has been reported to have better performance over the widely used P3HT polymer for gas sensing applications [33], [68], [136] as discussed in details in the literature review

of Chapter-1. In view of the above, the present chapter reports a PQT-12 polymer based MSM device with an Au-interdigitated electrode structure for sensing NH_3 and NO_2 gases. The proposed sensor is a resistor-type gas sensor fabricated on flexible polyamide substrate by the spin-coating method. The outline of the rest of this chapter is as follows:

Section 2.2 presents the experimental details of the fabrication of flexible MSM sensor. The results and discussions related to the film characterizations and NH_3 as well as NO_2 gas detections are included in section 2.3. Finally, section 2.4 has been used to conclude the objectives and outcomes of the research carried out in this chapter.

2.2 Experimental Details

2.2.1 Materials and Thin Film Deposition

The polymer PQT-12 purchased from American Dye Source Inc., Canada (ADS12PQT, Lot#14K007A1, molecular weight =23,000, polydispersity = 5.1 having HOMO = 5.24 eV & LUMO = 2.97 eV) has been used as an active semiconductor for sensor fabrication without any further purification. Highly pure NH_3 and NO_2 gas (99.99%) without any carrier gas have been purchased from the Sigma-Aldrich (India) and used without dilution to any carrier gases in the present study. Any other chemicals are purchased from Merck (India) and Sigma-Aldrich (India). The 25 μm thin polyamide sheet is used as the flexible substrate and PQT-12 thin film is deposited upon it. The flexible polyamide substrates are cut in a dimension of 20 mm × 15 mm and cleaned thoroughly using standard wet chemical cleaning procedures [153]. The cleaned substrates are dried in the oven at 100°C with the flow of nitrogen gas to make the surface more adhere to the polymer film. For the deposition of the active semiconductor layer, 5 mg PQT-12 is dissolved in 1 ml chloroform, and the solution is continuously

stirred at 70°C before the deposition. The PQT-12 solution is deposited on the polyamide substrate by the spin-coater. The film is coated at 2000 rpm for 40 seconds, and a thickness of 80 nm is achieved. After coating the film, it is dried at an optimized temperature of 80°C in the oven with the flow of nitrogen gas. The obtained PQT-12 thin film on polyamide substrates are characterized using XRD, SEM, and AFM measurements. The similar deposition conditions are taken for the preparation of other thin film samples of PQT-12 for FTIR and cyclic voltammetry on glass and ITO coated glass substrates, respectively.

2.2.2 Device Fabrication

The horizontal metal-semiconductor-metal (MSM) structure with PQT-12 as an active material is considered in the present study for gas sensing application. The interdigitated gold (Au) electrode is taken as metal part of the MSM for the formation of ohmic contact with the PQT-12 polymer. The band diagram in Figure 2.1 shows that the Au electrode makes ohmic contact with PQT-12 polymer films. For the formation of 50 nm thin Au electrode, the PQT-12 coated polyamide sample is loaded in the thermal evaporation chamber (model smart coat 3.0A from Hind High Vacuum, India). The active layer between these two interdigitated electrodes of the as-fabricated sensor is of 50 µm wide and 18 mm in length as shown in Figure 2.2 (a). The optical image of the fabricated sensor is shown in Figure 2.2 (b). The fabricated sensor can fold easily and shows a very good flexibility as shown in Figure 2.2 (c).

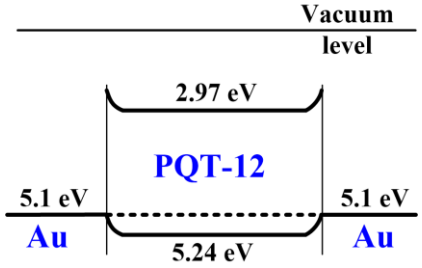

Figure 2.1: The band alignment of PQT-12 polymer with Au.

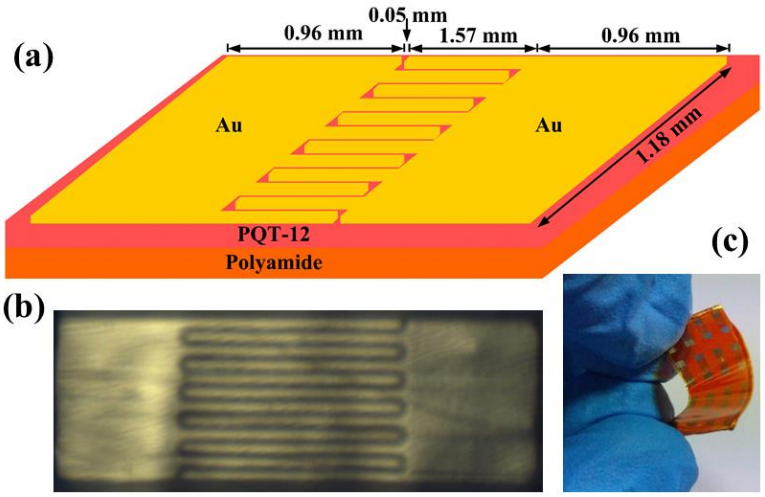

Figure 2.2: (a) Device structure of MSM sensor on polyamide substrate, (b) Optical image of as-fabricated sensor, and (c) Flexibility of as-fabricated sensor.

2.3 Results and Discussion

In this section, thin film and electrical as well as gas sensing characterization of PQT-12 based devices are presented.

2.3.1 Thin Film Characterization

The thin film XRD of the spin-coated PQT-12 film on polyamide substrate is obtained as shown in Figure 2.3. Two diffraction peaks at $2\theta = 7.4°$ and $21.4°$ are obtained which is arising from side-chain ordering and π-π^* stacking, respectively [30], [31] as shown in Figure 2.3. The amorphous PQT-12 thin film has a small crystalline peak for (300) at $2\theta = 15.0°$. The obtained XRD is due to low-temperature drying of the thin film. The unexpected elevation in the baseline in Figure 2.3 for low 2θ values, also observed by others [154], may be attributed to the instrumental limitation. The PQT-12 film roughness is calculated from AFM image shown in Figure 2.4. The average roughness, RMS roughness, peak-to-peak spacing, average grain size, and grain length estimated using Nova PX software are 0.6, 0.7, 6.4, 32.1, and 53.4 nm, respectively for the PQT-12 film on polyamide substrate. These parameters confirm that the film has

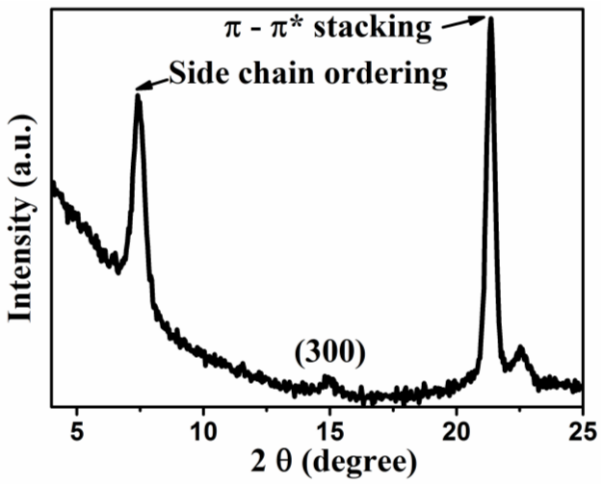

Figure 2.3: Thin film XRD of PQT-12 on flexible polyamide substrate.

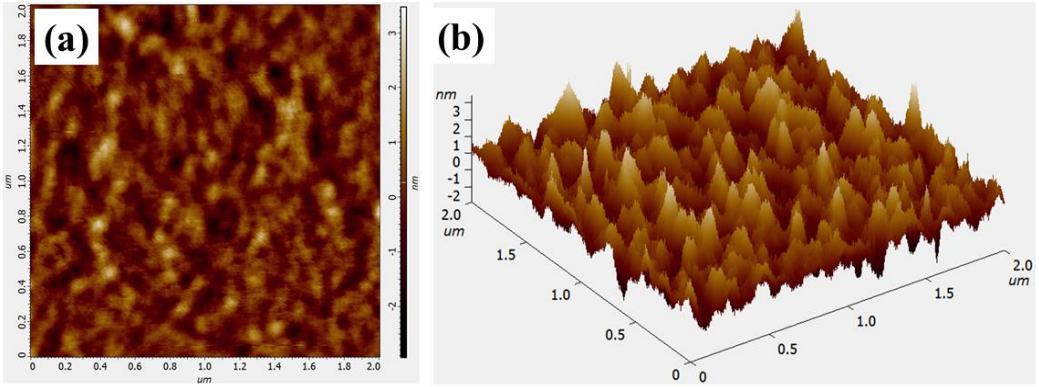

Figure 2.4: AFM topography of PQT-12 thin film on polyamide substrate: (a) 2 D and (b) 3 D.

nano-level roughness, which is good for fast recovery and better sensor performance [112].

The surface morphology of the PQT-12 film is studied using SEM images as shown in Figure 2.5. The SEM image of the PQT-12 film on carbon tape is taken to analyze the surface morphology as shown in Figure 2.5 (a). The obtained structured morphology is supported by carbon tape surface. The SEM image shows a highly smooth film of PQT-12 on polyamide substrate as shown in Figure 2.5 (b) as in [155]. The nano-level roughness observed on this highly smoothed PQT-12 film results in the stable sensor with fast response and recovery, whereas high roughness is desired for high gas response [74].

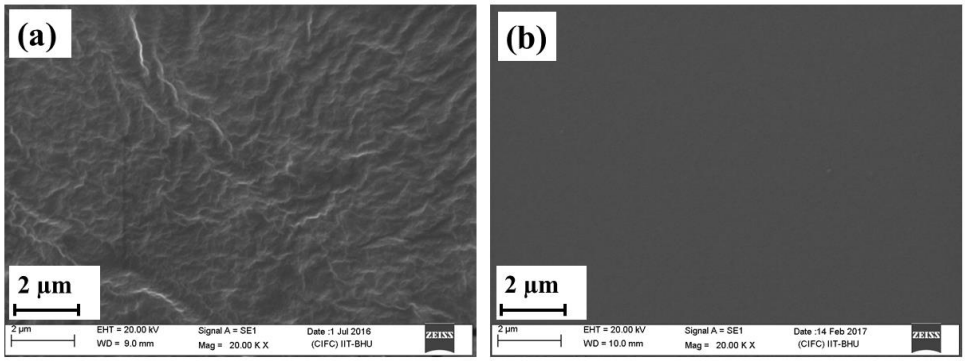

Figure 2.5: SEM image of PQT-12 film on (a) Carbon tape and (b) Polyamide substrate.

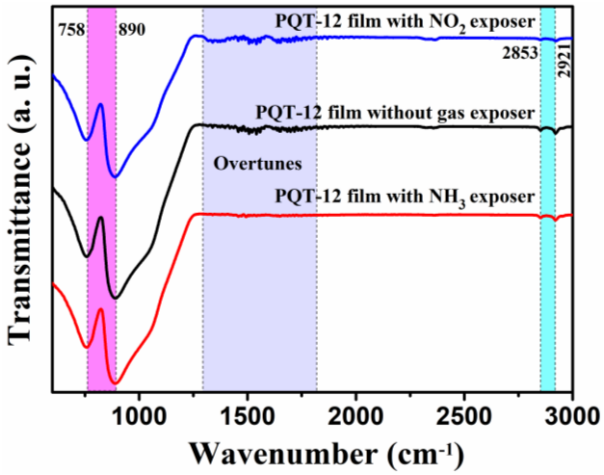

Figure 2.6: FTIR plot of the PQT-12 films: before gas exposure and after NH_3 and NO_2 gas exposure.

The FTIR measurements carried out in the transmittance mode for the PQT-12 films: before gas exposure and after the NH_3 and NO_2 gas exposure have been compared in Figure 2.6. The peaks for the aromatic ring observed at 758 and 890 cm^{-1} are resulted from the out of plane =C-H bending while the alkyl chain –C-H stretching vibration is observed at 2853 and 2921 cm^{-1} for the unexposed PQT-12 film [156]. The aromatic ring peaks observed to be negligible shifted with NH_3 and nitrogen gas absorption, similarly, the alkyl chain peak also shows shifting for NH_3 and NO_2 absorption. The NH_3 and NO_2 gas molecules disturb the thiophene ring, but after the recovery, the peaks of the PQT-12 molecule regain its initial state by discarding gas molecules from polymer ring [74]. This suggested that the chemical bonding and compositions of PQT-12 remain same after removal of gases.

For the cyclic voltammetry (CV) measurements, three electrodes namely Ag/AgCl as a reference electrode, platinum as a counter electrode and spin coated PQT-12 film on indium-doped tin oxide (ITO) as working electrode are used. The 0.1 M solution of tetrabutyl ammonium perchlorate (TBAP) in acetonitrile is used as an electrolyte for CV measurement. The scanning rate used is 50 mV in the range from 0.0 to 1.5 V [112]. The reduction and oxidation peaks in the PQT-12 film without gas exposure are observed at 1.09 V and 1.02 V, respectively [157] as shown in Figure 2.7. The HOMO level is estimated using the equation $E_{HOMO}(eV) = -e(E_{p'} + 4.65\,V)$, where $E_{p'}$ is the onset potential for oxidation relative to the Ag/AgCl reference electrode [158]. The value of $E_{p'}$ is calculated as 0.62 V and so the $E_{HOMO} = 0.62 + 4.65 = 5.27\,eV$. The higher value of the HOMO level than the regioregular P3HT confirms the high stability of the PQT-12 film in the as-fabricated sensor [157]. The CV characteristics shown in Figure 2.7 of the PQT-12 film after NH_3 exposure shows the same trace of the curve as without gas exposure, whereas after NO_2 exposure the CV characteristic is change and the peaks are eliminated due to oxidation of PQT-12 surface by NO_2 gas.

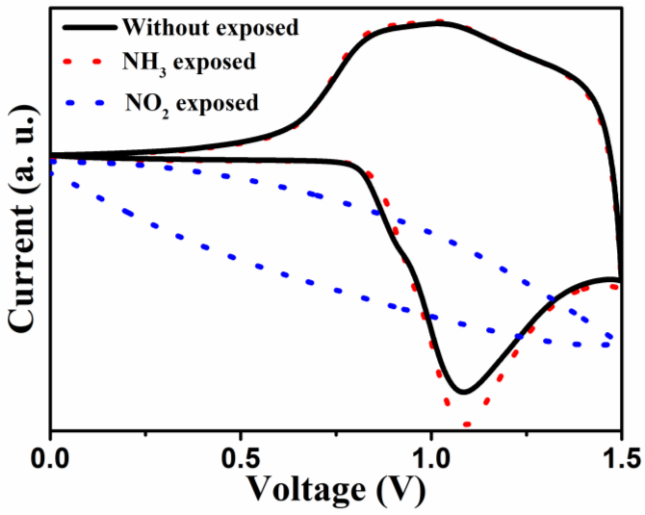

Figure 2.7: CV plot of the PQT-12 films: without gas exposure and with NH_3 and NO_2 gas exposed.

2.3.2 Electrical Characterization

The current-voltage (*IV*) characteristics of the PQT-12 based interdigitated MSM sensor under study have been shown in Figure 2.8. The perfect linear *IV* characteristic is obtained due to the formation of ohmic contact between PQT-12 and Au. The logarithmic scale of the *IV* characteristics is shown in the inset of Figure 2.8. The stability of the fabricated sensor is also investigated in an ambient air environment. Figure 2.9 shows the sensor stability curve over 10 days. The MSM sensor shows a less

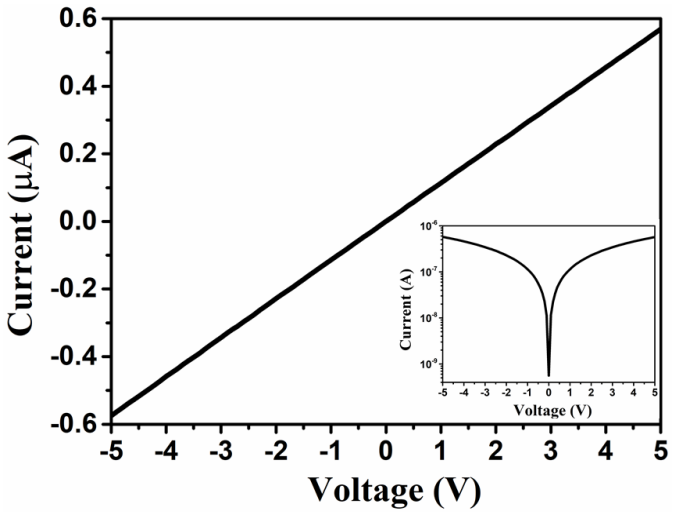

Figure 2.8: *IV* characteristics of interdigitated MSM sensor under dark and unexposed condition. Inset shows the logarithmic current scale.

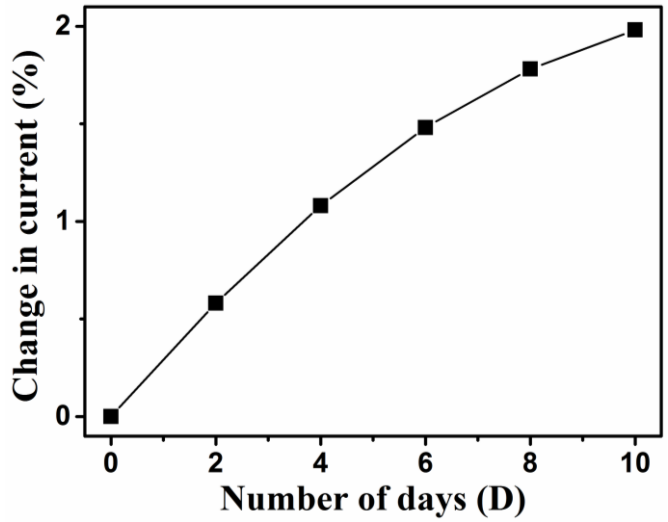

Figure 2.9: Stability characteristics of the MSM sensor over 10 days.

than 2% decrease in current due to moisture and oxygen in the atmosphere (or due to environmental NH_3).

2.3.3 Gas Sensing Characterization

The gas sensing characteristics of flexible MSM sensors have been performed under a dark condition in the homemade gas sensing chamber at room temperature (~23˚C) and 56% relative humidity (RH) conditions. The sensor is placed in the sensing chamber to measure the change in the *IV* characteristics with the exposure of various gases/concentration. The sensor performance parameter, the gas response is defined as [159]:

$$S(\%) = \frac{I_o - I_g}{I_o} \times 100\,\% \tag{2.1}$$

where, I_o and I_g are the sensor current before and after gas exposure, respectively. The ± sign in Equation (2.1) depends on the type of gases, whether they are reducing or oxidizing gases. When reducing gases are exposed to the p-type polymer, the resistance of the thin film is increases and current decreases. So, the + sign is taken. Whereas with exposure of oxidizing gases, the resistivity decreases and current increases; so negative sign is taken.

The PQT-12 film has an assembled collection of molecules along with a large number of charge carriers and few traps as shown in Figure 2.10 (a). Note that the NH_3 gas sensing mechanism of polythiophene-based sensors is elucidated by base de-doping and dipole-charge interaction [77], whereas NO_2 gas sensing can be explained by the change of conductivity of the polythiophene film due to the modulation of redox levels and partial positive charge transfer to the film by the electronegativity of the NO_2 gas [40]. Therefore, the trap charges in the PQT-12 molecule are increased and hole concentration is decreased with exposure of NH_3 gas as shown in Figure 2.10 (b),

whereas the trap charges reduced and hole concentration are increased with exposure of NO_2 gas as shown in Figure 2.10 (c).

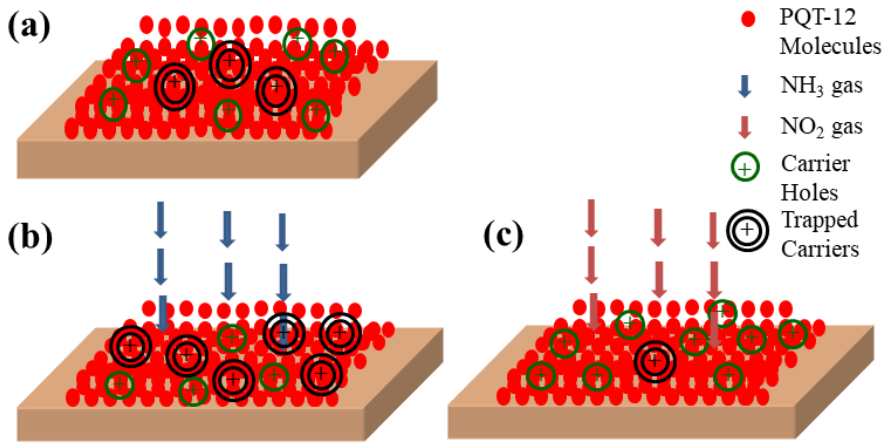

Figure 2.10: (a) Assembled layer of PQT-12 film with molecules, carrier holes, and trapped carriers, (b) PQT-12 film after exposure to NH_3 gas, and (c) PQT-12 film after exposure to the NO_2 gas.

2.3.3.1 Ammonia Gas Response of MSM Sensor

The current-voltage characteristics of the PQT-12 based MSM ammonia sensor under study have been shown in Figure 2.11 without and with 100 ppm NH_3 gas exposure conditions. Since NH_3 behaves as an electron donor and basic in nature, NH_3 gas starts doping and de-doping in the PQT-12 film when it is exposed to NH_3 gas [72], [75]. This results in the formation of increased traps on the surface of the film demonstrated in Figure 2.10 (b). Due to increased trapped carriers, the charge carriers are reduced and hole mobility is decreased. As a result, the film resistivity is increased with the absorbed NH_3 in the PQT-12 film.

The gas response to the NH_3 gas over 10 to 100 ppm concentrations at an applied voltage of 5 V is calculated using Equation (2.1) and the response transient of the sensor is shown in Figure 2.12. Clearly, a proportional change in the gas response is observed which is slightly saturated at higher concentration of NH_3 gas. However, a slight drift in the response baseline observed as shown in the transient response in Figure 2.12 is

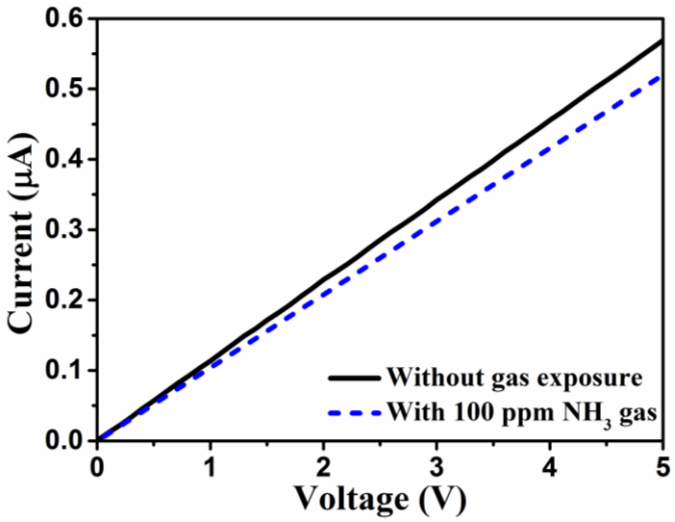

Figure 2.11: The current-voltage characteristics of the PQT-12 based MSM ammonia sensor without and with a 100 ppm NH_3 gas exposure conditions.

attributed either to the trace of trap sites remaining in the PQT-12 film while desorption of NH_3 gas during recovery period or to the moisture and oxygen [160] present in the atmosphere.

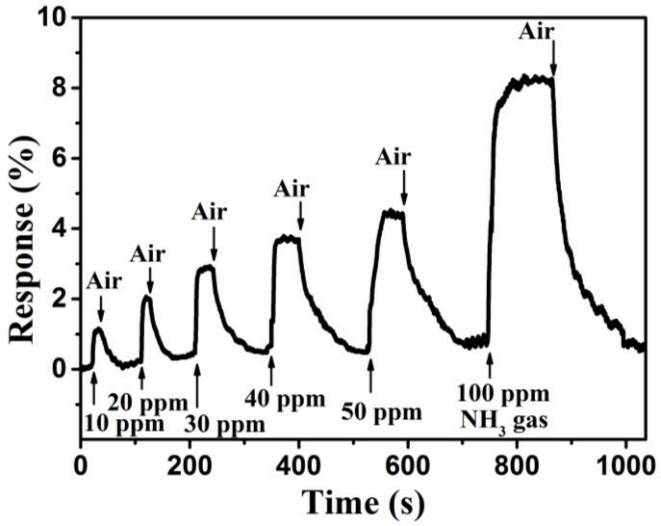

Figure 2.12: The gas response transient of the sensor at an applied bias of 5 V with NH_3 gas exposure.

A gas response of 8.6% has been observed for 100 ppm of NH_3 gas. This larger response than the reported value by Vieira et al. [67] is attributed to the optimized PQT-12 film on polyamide substrate and larger effective gas exposed area with an increased width to length ratio. The response is good enough to detect the 100 ppm of NH_3 which can start irritation in the eyes and can be fatal. The response time (T_{res}) and recovery

time (T_{rec}) defined as the time required for changing the response from 0 to 90% immediately after exposing to the NH_3 gas and 100 to 10% immediately after the removal of the gas, respectively [161]. The T_{res} and T_{rec} for 100 ppm of NH_3 are determined as 8 s and 103 s, respectively. The faster T_{res} and T_{rec} as compared to those reported by Dai et al. [33] are attributed to the highly smooth PQT-12 film with nano-level roughness (see Figure 2.4 and 2.5) and larger effective exposed area with an increased width to length ratio of the as-fabricated MSM sensor structure under study.

The gas response is nearly linear with NH_3 gas concentration which is linearly fitted as $y=0.081x+0.595$ with a correlation coefficient, $R^2=0.999$ is shown in Figure 2.13, where y is a gas response in percentage and x is NH_3 concentration in ppm. The slope of the response and concentration plot is called the sensitivity of the gas sensor [159] which is determined as 8.1×10^{-4} ppm^{-1}. Using the noise theory of ref. [162], the sensor noise defined as the root mean square deviation (rmsd) is determined as 8.1×10^{-5}. Assuming that the signal-to-noise ratio is greater than 3 for any real signal, the detection limit (DL) of the proposed sensor can be expressed as [162]:

$$DL(ppm)=3\frac{rmsd}{sensitivity} \tag{2.2}$$

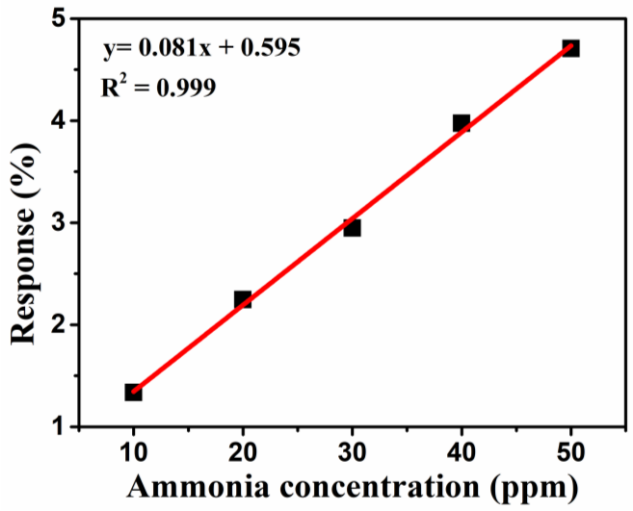

Figure 2.13: Responses at different concentration of NH_3 gas with linearly fitted.

The sensor detection limit for the NH_3 gas is estimated as 300 ppb. This lower value of the detection limit may be attributed to the smoother film surface and higher stability of PQT-12 in the air [31].

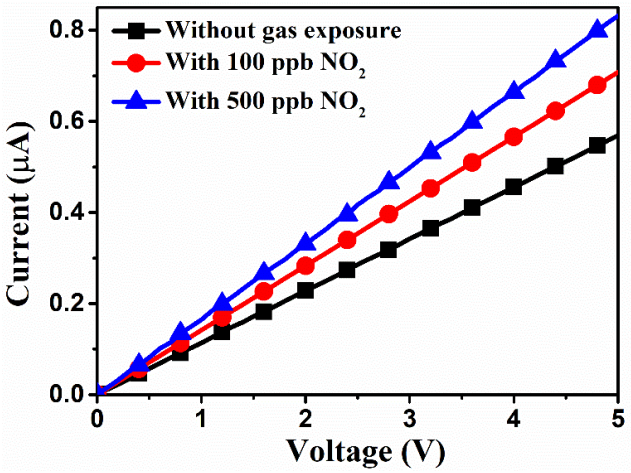

Figure 2.14: The sensor current-voltage characteristics: before gas exposure and after exposure of 100 ppb and 500 ppb of NO_2 gas.

2.3.3.2 Nitrogen Dioxide Gas Response of MSM Sensor

The room-temperature *I-V* characteristics of the PQT-12 based MSM sensor under ambient and NO_2 gas exposure of 100 ppb and 200 ppb have been shown in Figure 2.14. The increase in current with the NO_2 gas concentration can be explained by the change of conductivity of the PQT-12 film due to the modulation of redox levels and partial positive charge transfer to the film by the electronegativity of the NO_2 gas [40]. The difference between the redox level of the PQT-12 molecule and NO_2 gas causes the charge transfer from the film to the gas depending on their redox levels. This charge transfer reduces the trapped charges present in the polymer film thereby donating positive charges to the polymer. Since the PQT-12 is inherently a p-type semiconducting polymer, the transferred positive charges enhance the overall hole concentration [58] and hence the conductivity of the PQT-12 film. In addition to the above phenomenon, the adsorption kinetics of gas on the PQT-12 polymer film is also

responsible for NO_2 gas sensing [40] of the sensor under study. This increased film conductivity with NO_2 exposure is responsible for the increased sensor current in Figure 2.14.

The transient response of the PQT-12 based MSM sensor at 5 V bias voltage is shown in Figure 2.15 for different NO_2 gas concentrations over 100-500 ppb. Since the sensor is expected to be in air in practice and the PQT-12 has better stability in air than other polymers [33], the recovery characteristics shown in Figure 2.15 are measured under air. The gas response and response time of the sensor for 100 ppb NO_2 gas are found to be ~24% and ~41 s, respectively, whereas large recovery time is observed as seen from Figure 2.15. The gas responses for 100 ppb and 500 ppb NO_2 gas concentrations have been compared in the inset of Figure 2.15. The gas response is found to be increased from ~24% to ~48% with the increase in the NO_2 gas concentration 100 ppb to 500 ppb which gets slightly saturated at 500 ppb. Note that the gas response of ~48% is reasonably good and comparable to the P3HT polymer-based gas sensors [58]. It may be observed that a significant change in current is observed in Figure 2.14 with increase in the concentration from 100 ppb to 500 ppb while nearly no change in the response transient is observed in Figure 2.15 for the same successive increase in the gas concentration. This can be explained as follows: Each time the film is exposed to the NO_2, the chemisorption of oxidizing NO_2 gas damages the surface of the film. Note that the gas concentration was increased directly from 100 ppb and 500 ppb for current measurements in Figure 2.14, while the concentration of 500 ppb was increased after exposing the device with concentrations of 100 ppb, 200 ppb, 300 ppb and 400 ppb for response measurements in Figure 2.15. Thus, the change in surface morphology of the PQT-12 film in the sensor is expected to be more in case of response measurements than that of the film used for current measurements with 500 ppb NO_2

concentration. In brief, the incomplete recovery of the PQT-12 based MSM sensor under study due to the extensive oxidising nature of the NO_2 gas [58] is responsible for the insignificant increase in the response transient despite the successive increase in concentration up to 500 ppb as observed in Figure 2.15. The calibration curve (Gas response versus NO_2 concentration) is plotted in Figure 2.16 using the results obtained from transient characteristics. The plot is nearly linear with a correlation coefficient, $R^2 = 0.99$. The theoretical detection limit [163] of the sensor is calculated as 32 ppb.

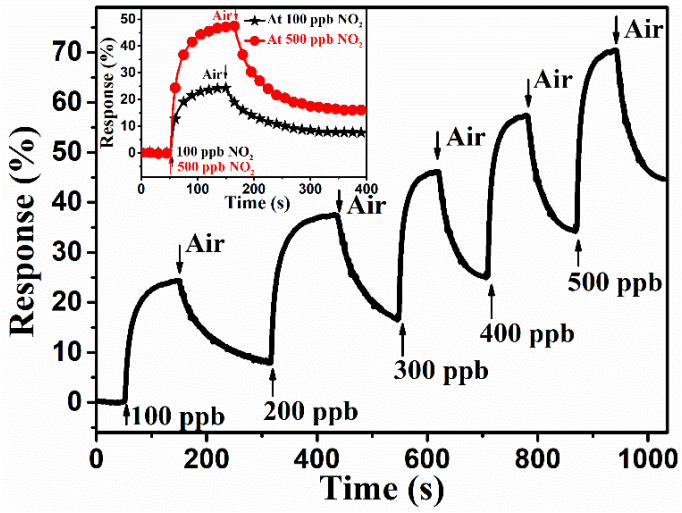

Figure 2.15: Transient gas responses of MSM sensor at 5 V with 100 to 500 ppb of NO_2 gas exposure. The transient responses at 100 and 500 ppb of NO_2 gas are in the inset of figure.

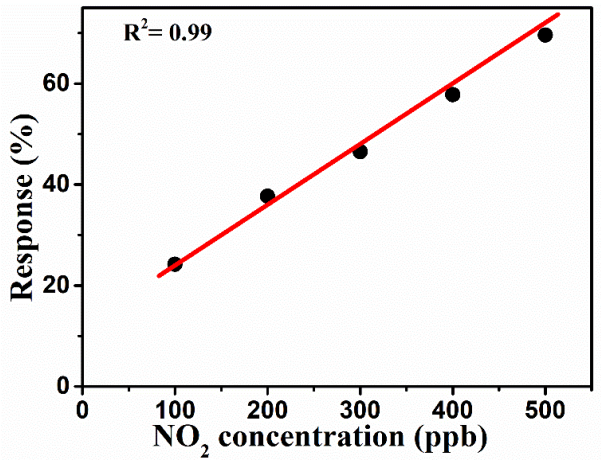

Figure 2.16: Linearity plot of the obtained NO_2 gas response of the sensor.

2.3.3.3 Selectivity of MSM Sensor

The selectivity of the as-fabricated PQT-12 based MSM sensor has been investigated in the presence of ammonia, nitrogen dioxide, carbon monoxide (CO) and the most common solvent gases/vapours such as methanol and acetone. Methanol vapours naturally present with a small amount in the atmosphere breaks into CO_2 and water (which is analogous to water vapour) in the sunlight. Acetone is present in human and animal waste along with NH_3. The gas response of NH_3 and NO_2 gases at an applied voltage of 5 V is much higher than the CO, methanol and acetone as shown in Figure 2.17. It is important to note that the sensor current is increased significantly with the NO_2 gas concentration while it is decreased with the increased NH_3 gas concentration. The effect of relative humidity (RH) (at 23°C) on the as-fabricated PQT-12 based MSM sensor demonstrated in Figure 2.18 shows a small increase in the current

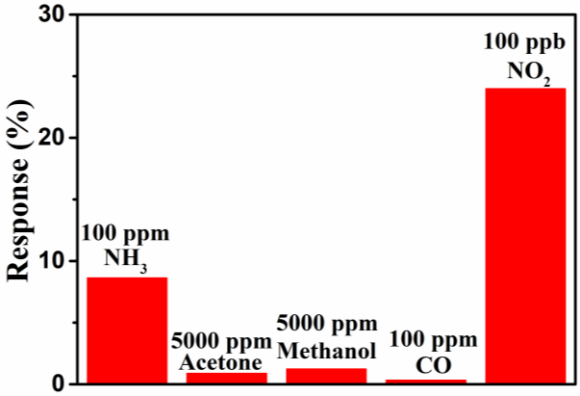

Figure 2.17: Selectivity plot of the MSM sensor in presence of interfering gases and organic vapours.

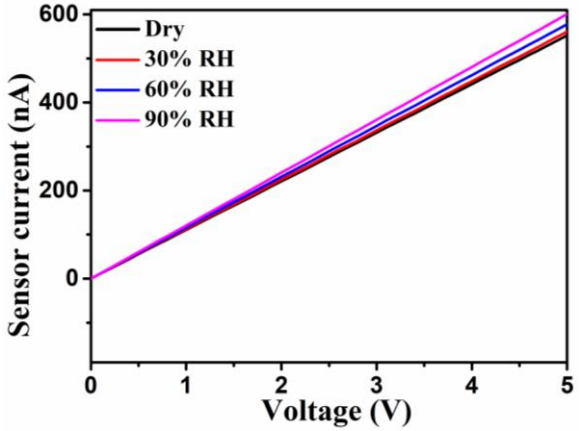

Figure 2.18: The current-voltage characteristics of MSM sensor at different relative humidity values.

with an increased percentage of RH which is insignificant as compared to that obtained with the exposure of NH_3 and NO_2 gases.

2.4 Conclusion

In this chapter, a flexible organic thin film MSM structure with interdigitated electrodes is fabricated on a polyamide substrate using PQT-12 conducting polymer for NH_3 and NO_2 gas detection applications. The PQT-12 films have been grown on the flexible polyamide substrate using spin-coating method. The morphological and structural characteristics of the PQT-12 films have been analyzed by using XRD, AFM, SEM, FTIR and CV measurement data. The NH_3 sensing characteristics have been measured for a wide range of NH_3 concentrations of 10 ppm - 100 ppm. The NH_3 gas sensing mechanism of the PQT-12 based MSM sensor is observed to be dominated by the base de-doping and dipole-charge interactions. A response of as high as 8.6% for 100 ppm NH_3 and a detection limit of 300 ppb are obtained at room temperature and a low applied voltage of 5 V. The sensor shows a faster response time of 8 s and recovery time of 103 s for NH_3 gas. The principle of NO_2 gas sensing is based on the change in the conductivity of PQT-12 film of the MSM device resulted from the transfer of partial positive charges to the film by the electronegativity of the NO_2 gas. The proposed MSM sensor shows a gas response of ~24% with a response time of ~41 s measured for 100 ppb of NO_2 gas. The gas response is increased with the gas concentration with the maximum gas response of ~48% at 500 ppb NO_2 gas. The sensor has a detection limit of 32 ppb for NO_2 gas. The gas response of MSM sensor is reasonably good at low bias operation for detecting low-concentration of NO_2 gas. However, the gas response for NH_3 gas at 100 ppm is relatively low and hence requires further improvement by film/device engineering.